Available online at www.sciencedirect.com
SCIENCE DIRECT®
Polymer 44 (2003) 8033–8040
polymer
www.elsevier.com/locate/polymer

The interfacial properties and porous structures of polymer blends characterized by synchrotron small-angle X-ray scattering

Jing Wu*

Otto H. York Department of Chemical Engineering, New Jersey Institute of Technology, Newark, NJ 07102, USA

Received 1 April 2003; received in revised form 17 September 2003; accepted 18 September 2003

Abstract

Microvoids are induced upon uniaxial drawing of films made from immiscible polypropylene (PP)/polystyrene (PS) binary blends and ternary blends of PP, PS, and a block copolymer SEEPS. The shape of the uniaxially oriented microvoids is rod- or slit-like with a high aspect ratio. Synchrotron small-angle X-ray scattering (SAXS) is used to characterize the dimensions of these microvoids. Their scattering image is an intense azimuthally narrow equatorial streak on a two-dimensional SAXS pattern. This streak is analyzed to obtain the diameter, length and misorientation of the microvoids. The microvoids length is identified as an effective measure of the interfacial adhesion and strength between phase domains. Drawn films of binary blends of PP/PS are found to have the longest microvoids. The initial addition of the block copolymer SEEPS as a compatibilizer enhances the interfacial adhesion and shortens the length of microvoids. Further addition of compatibilizer induces the formation of aggregates of a composite PS/SEEPS dispersed phase, and this leads to reduced interfacial adhesion and a longer microvoids. Interfacial properties are also dependent on the mixing protocol used to produce the blends.

The transport property of the films is determined by porosity and the degree of interconnectivity. A convenient measure of the degree of interconnectivity is proposed. The degrees of interconnectivity of these films are in accordance with the interfacial adhesion and strength. Non-equatorial streaks are observed and attributed to the microvoids with a complex orientation and geometry, which are responsible for the interconnectivity among microvoids.

Keywords: Membranes with elongated microvoids; The degree of interconnectivity; Equatorial streaks and streaks around the beamstop without an equatorial orientation

1. Introduction

Blending of different polymers is an important and efficient strategy to tailor desired properties of polymer systems. It is for this reason that a large body of literature on polymer blends has emerged [1]. As most polymers are incompatible, modification of the interface of polymer blends to fine tune interfacial properties is of great importance. In applications where mechanical properties are of a major concern, good adhesion across the interface is desired. In other applications, a delicate balance on interfacial properties is required. One such example arises from the solvent-free fabrication of polymer films with a potential as membranes via uniaxial drawing of immiscible polymer blends [2–4]. In this application, the goal is to control phase morphology and interfacial adhesion of polymer blends so that interconnecting microvoids can be induced upon uniaxial drawing. The microvoids formation mechanism is identified as crazing along the phase boundaries as a result of the uniaxial drawing [2,4]. The shape of the resulting microvoids is rod- or slit-like with a high aspect ratio. The dimensions of the uniaxially oriented microvoids induced by the same drawing conditions in polymer blends not only are of great implications for membrane properties, but also represent the interfacial adhesion and strength of the blends. Therefore, an accurate measurement of microvoids dimensions is of immense value for both scientific and application purposes.

Small-angle X-ray scattering (SAXS), which has been widely used to study polymer and colloidal systems, is an indispensable tool for investigation of nanoscale heterogeneities of electron density [5]. In a microvoids-bearing polymer system, electron density contrast arises between polymer (either crystalline or amorphous) and microvoids,

* To whom all correspondence should be addressed.
E-mail address: jingwu@adm.njit.edu (J. Wu).

0032-3861/$ - see front matter © 2003 Elsevier Ltd. All rights reserved.
doi:10.1016/j.polymer.2003.09.059

and possibly between crystalline and amorphous phases. Since the SAXS intensity is proportional to the square of the electron density difference between adjacent domains, the scattering from microvoids typically accounts for 97–99% of the overall scattering in semicrystalline polymers [6,7]. The scattering from microvoids dominates the SAXS scattering patterns, and in most situations the scattering can be regarded as originated exclusively from microvoids even if there exist other heterogeneities. Therefore, SAXS is an ideal tool to characterize nanoscale microvoids.

The two-dimensional (2D) SAXS pattern from polymers containing rod-like microvoids is a diffuse equatorial streak. There has been a long history of investigation on this diffuse equatorial streak from polymer fibers. In 1950s, Statton [8,9] first ascribed the equatorial streak on SAXS patterns from cellulose fibers to microvoids. This diffuse streak was further studied by Ruland and coworkers from carbon fibers [10–12] in the 1970s. More recently, this equatorial streak has been reinvestigated by Grubb and coworkers [6], Murthy et al. [13,14] and us [7], as well as many others [15–17] in polymer fiber systems. Among these contributions, Ruland and Perret [10–12] and Grubb and Prasad [6] formulated kinematical approaches to analyze the equatorial scattering streak to evaluate the dimensions of the elongated microvoids. In 1980s, Tang, Fellers and Lin showed that scattering from microvoids might need dynamical scattering analysis, and developed a vector scattering theory [18]. While the dynamical scattering approach is more rigorous, the kinematical approach, which is used by many researchers, is a satisfactory approximation for the analysis of scattering from microvoids.

In this article, the dimensions of uniaxially oriented microvoids induced in films of immiscible polymer blends upon drawing are evaluated using the kinematical approach developed by Grubb and Prasad [6]. The length of the microvoids is correlated to the composition and the mixing protocols of the blends, and is demonstrated to be a convenient measure of interfacial adhesion and interconnectivity among microvoids. Another type of streaks around beamstop, but not equatorially oriented, is attributed to microvoids with a complex orientation and geometry, providing interconnectivity among microvoids.

2. Experimental

The films are fabricated by uniaxial drawing of immiscible polymer binary and ternary blends. The details of the manufacture of these films can be found elsewhere [2–4]. Briefly, the binary blends are produced via melt compounding of polypropylene (PP) (PF-100, Montell), and polystyrene (PS) (Styron 685D, Dow Chemicals) at a ratio (wt%) of 90/10 in a 27 mm diameter intermeshing co-rotating twin-screw extruder. The ternary blends are produced via mixing of the same PP, PS, and a triblock copolymer, hydrogenated polystyrene-*block*-polybutadiene-*block*-polyisoprene-*block*-polystyrene, commercially known as SEEPS, (Kuraray America) at ratios (wt%) of 90/10/5 and 85/15/7.5. Two mixing protocols are used to produce the ternary blends. The one-step mixing compounds three components in one step by simultaneously introduced them into an extruder. In the two-step mixing, the PS and the copolymer SEEPS are premixed in a co-rotating twin-screw extruder prior to mixing with PP. The microvoids-bearing films are obtained by uniaxial drawing (up to 500%) the nonporous precursor films, which are produced by extruding the pellets of the binary and ternary blends through a 10 cm flat sheet die. The drawing temperature is 50–75 °C, about 25–50 °C below the glass transition of PS in order to prevent the deformation of the PS phase. The symbol for each film, its composition, and the corresponding mixing protocol are listed in Table 1.

Synchrotron SAXS measurement is carried out at the Beamline X3A2 of the National Synchrotron Light Source, Brookhaven National Laboratory ($\lambda = 1.54$ Å, beam diameter = 300 μm). The primary X-ray beam is monochromatized by a double single crystal monochromator. The wavelength spread is less than 0.01%. During the SAXS experiment, the incident X-ray is perpendular to the film with the draw direction vertical. 2D SAXS scattering patterns are recorded by Fuji™ HR-V imaging plates. The sample to detector distance is 1137.25 mm. The imaging plates are digitized by a Fuji™ BAS 2000 scanner with a resolution of 100 μm. A typical collection time is 2 min. The recorded SAXS patterns or their corresponding one-dimensional extracted profiles are subject to incident beam intensity, scattering volume and background corrections.

3. Data analysis

A representative 2D SAXS pattern from the binary blends PP/PS-90/10-1 is shown in Fig. 1. From this pattern, one observes an intense azimuthally narrow equatorial streak. Collection time has to be controlled within 2 min in order not to saturate the imaging plate. SAXS patterns from other ternary blends also bear this intense equatorial streak. Because of the reciprocal scattering law, the equatorial steak

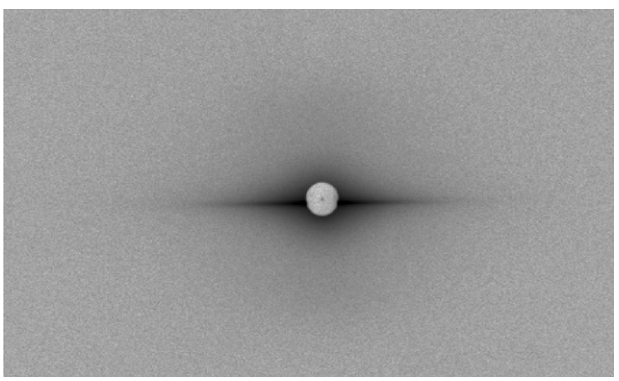

Fig. 1. A two-dimensional small-angle X-ray scattering pattern from PP/PS binary blends, PP/PS-90/10-1.

Table 1
The composition and the mixing protocols used to fabricate the films of immiscible polymer blends

Line #	Symbol	Composition	Ratio (wt%)	Mixing protocol
Line 1	PP/PS-90/10-1	PP/PS	90/10	One-step
Line 2	PP/PS/SEEPS-90/10/5-1	PP/PS/SEEPS	90/10/5	One-step
Line 3	PP/PS/SEEPS-90/10/5-2	PP/PS/SEEPS	90/10/5	Two-step
Line 4	PP/PS/SEEPS-85/15/7.5-2	PP/PS/SEEPS	85/15/7.5	Two-step

represents scattering from elongated rod- or slit-like entities with a high aspect ratio. For the patterns collected in this work, given the extremely high intensity of the equatorial streak, the scatterers are identified to be elongated microvoids. The corresponding scanning electron micrograph (SEM) shown in Fig. 2 [2] also suggests the existence of elongated microvoids. Although the diameter of the microvoids may be extracted from an SEM [2–4], it is extremely difficult, if not impossible, to obtain the length and orientation of the elongated microvoids from an SEM. In order to evaluate the dimensions of the microvoids, the 2D synchrotron SAXS technique is employed. The resulting 2D SAXS patterns are analyzed by the following methods.

3.1. The diameter of microvoids

The diameter of the microvoids is obtained by least-square fitting an equatorial scan from a background corrected 2D SAXS pattern using the relationship for rod-like scatterers [5],

$$\ln I = \text{const} - \frac{q^2R^2}{4} \tag{1}$$

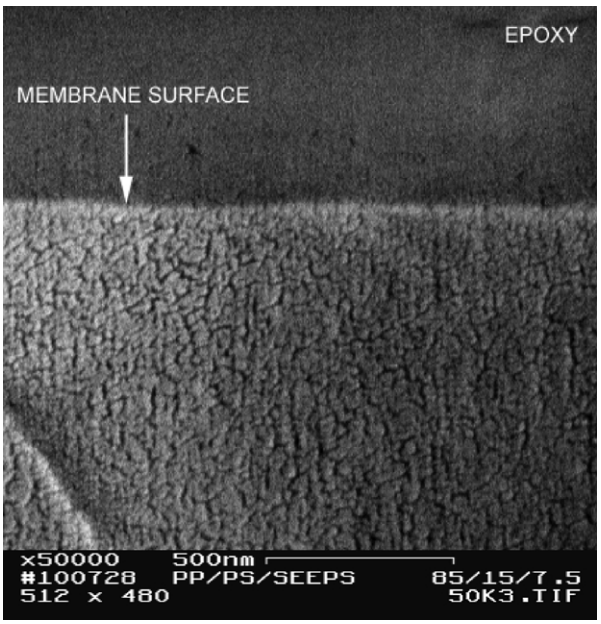

Fig. 2. Scanning electron micrograph of the cross-section of PP/PS/SEEPS blends, PP/PS/SEEPS-85/15/7.5-2 (from Ref. [2]).

3.2. The length and orientation of microvoids

In order to estimate the length and misorientation of microvoids, the method established by Grubb and Prasad [6] is adopted.

As shown in Fig. 3, longitudinal scans of the equatorial streak are taken perpendicular to the equator. The integral breadths (IB) of the sliced profiles are found to increase with the scattering vector along the equator (q_{12}). As shown by Grubb and Prasad [6], the IB of the longitudinal scans are due to size broadening, i.e. the effect of the limited length of the elongated scatterers, and due to the distribution of orientation of the elongated scatterers with respect to the draw direction. With the use of the common assumption that size broadening is Cauchy and the distribution of orientation is Gaussian, i.e. the C–G assumption, the following relationship is obtained Grubb and Prasad [6],

$$\frac{\text{IB}\cos(2\theta)}{\lambda D} = \frac{1}{2L} + \left[\frac{1}{4L^2} + \frac{q_{12}^2 \sin^2\beta}{4\pi^2}\right]^{1/2} \tag{2}$$

where $q = 4\pi \sin\theta/\lambda$ is the scattering vector and q_{12} is its component in the equatorial direction, 2θ is the scattering angle, λ is the wavelength of the X-ray, D is the sample to detector distance, and L and β are the average length and the misorientation angle of microvoids.

Alternatively, if both the size broadening and orientation distribution are Cauchy, i.e. the C–C assumption, IB depend on L and β according to the following relationship [6],

$$\frac{\text{IB}\cos 2\theta}{\lambda D} = \frac{1}{L} + \frac{q_{12}\sin\beta}{2\pi} \tag{3}$$

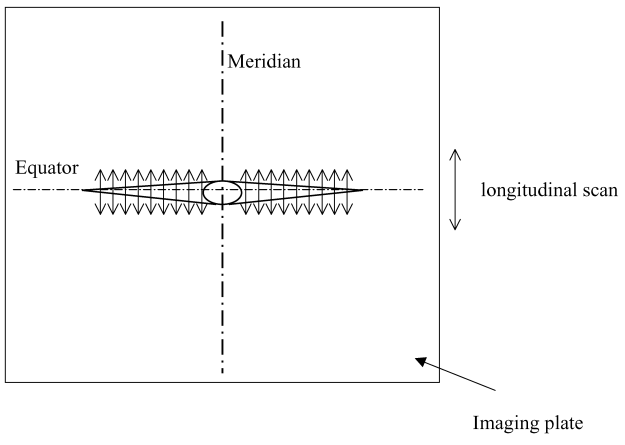

Fig. 3. A schematic representation of the Grubb's analysis.

To extract the length, L, and the misorientation angle, β, of the microvoids, longitudinal scans of an equatorial streak are first fitted with Lorentzian functions to obtain the IB of the sliced profiles. Fitting the sliced profile with the Lorentzian function is just a convenient and accurate numerical way to obtain the IB. It should not be construed as the C–C assumption is made. After obtaining the IB at each q_{12}, the common C–G assumption is made, and therefore, the microvoids length L and misorientation angle β are obtained by a nonlinear least-square Levenberg–Marquardt fit [19] of IB vs. q_{12} using Eq. (2).

The same approach, i.e. fitting the longitudinal scans with Lorentzian functions to obtain the IB, and then using Eq. (2) to evaluate L and β, had been used by Murthy et al. [14] to evaluate the length and misorientation of the elongated scatterers.

The fitted curve and the discrete data of IB vs. q_{12} are shown in Fig. 4 for all films studied in this research. The q_{12} range of a fit usually ranges from 0.0115 to 0.0250 inverse angstroms, corresponding to a real-space range of 25–63 nm. The q resolution of the beamline is 0.00045 inverse angstroms. The maximum real-space resolution of the experimental setup is estimated to be 600 nm, with the considerations of both the resolution in q and the effect of beamstop. This approach is in essence an extrapolation from the accessible q range to that corresponding to the range of microvoids length, c.a. 150–500 nm.

The microvoids length and misorientation are shown as legends in Fig. 4. The diameter, length and misorientation angle of the microvoids in each film are also listed in Table 2.

3.3. Other aspects of the analysis

The errors associated with the microvoids diameter, length and misorientation are originated from two sources: (a) the fitting process, and (b) the uncertainties in wavelength, IB (or pixel resolution of the imaging plates), sample-to-detector distance and scattering vector. The latter is the major source as all fitting runs coverges nicely and generate a negelibile amount of fitting error. To estimate the errors originated from the source (b), a standard error analysis is performed to account for the errors in microvoids diameter by differentiating Eq. (1), and to account for the errors in microvoids length and misorientation by differentiating Eq. (2). Since the error in microvoids length and misorientation are coupled, it is assumed that the errors in microvoids length and misorientation each account for 50% of the error generated from the source (b). The estimated errors are listed in Table 2 along with the corresponding results.

It is important to note that only kinematical scattering analysis (i.e. the Guinier's analysis for microvoids diameter and the Grubb's method for microvoids length and misorientation) is used to analyze the data. The scattering profiles can be fit nicely with the equations predicated by the

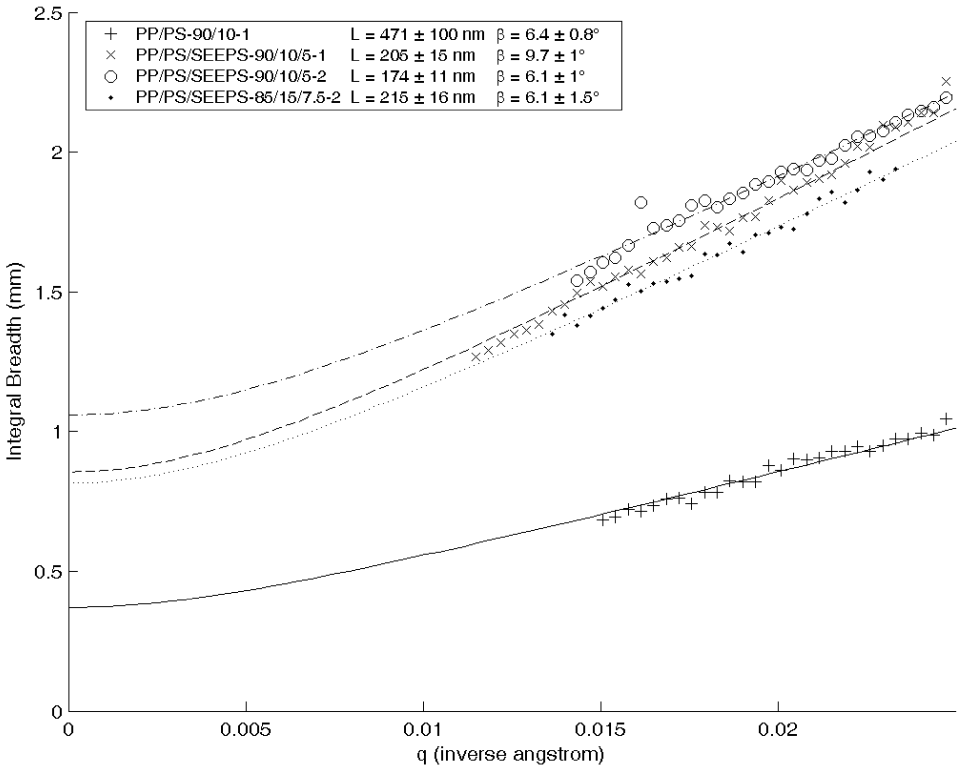

Fig. 4. The discrete data of IB vs. q_{12} and the fitted curve generated during the evaluation of the length and misorientation of the microvoids of each film studied. To eliminate the error introduced by the sensitivity difference of the pixel elements on an imaging plate, the original data from the right half of the equatorial streak ($q_{12} > 0$) is used.

Table 2
The dimensions of the microvoids in the films of immiscible polymer blends

Line #	Symbol	Length (nm)	Misorientation (°)	Diameter (nm)[a]	Diameter (nm)[b]
Line 1	PP/PS-90/10-1	471 ± 100	6.4 ± 0.8	15 ± 2	12
Line 2	PP/PS/SEEPS-90/10/5-1	205 ± 15	9.7 ± 1	14 ± 2	7
Line 3	PP/PS/SEEPS-90/10/5-2	174 ± 11	6.1 ± 1	13 ± 1	7.6
Line 4	PP/PS/SEEPS-85/15/7.5-2	215 ± 16	6.1 ± 1.5	14 ± 2	12.7

[a] From SAXS fitting of this investigation.
[b] From SEM imaging analysis, taken from Ref. [2].

kinematical theory. In addition, the void diameter obtained from the scattering method is well supported by the SEM data shown in Table 2. Therefore, the use of kinematical scattering analysis a good approximation, and the dynamical scattering analysis by Fellers, Lin and coworker is not used [18].

It is also necessary to point out that the scatterers, i.e. microvoids, are densely packed. Since microvoids are of a high aspect ratio, the effect of multiple scattering can be neglected [20]. In addition, the deconvolution of the beam profile is not performed for the longitudinal scans of the equatorial streak because the beam size is so small that the scattering can be regarded as from a point source.

4. Results and discussions

The diameter, length and misorientation of the microvoids in each film are listed in Table 2. By inspection, one finds that the microvoids diameter and misorientation are nearly independent of the composition and the mixing protocols. On the other hand, the length of the microvoids exhibits a strong dependence on the use of compatibilizer, the mixing protocol and hence the nature of the interface.

4.1. The effect of compatibilizer

The use of a compatibilizer is well known to reduce the interfacial tension and to enhance the interfacial thickness and adhesion [1,21]. The compatibilizer used in this research is nonreactive SEEPS triblock copolymer, composed of two hard glassy PS end blocks and a soft hydrogenated polybutadiene-*block*-polyisoprene midblock. The two PS end blocks of the SEEPS are expected to dissolve in the PS homopolymer domain, while the soft SEEPS midblock is expected to have a strong affinity to the PP homopolymers domains. This is supported by the reduction in interfacial tension and increase in interfacial thickness estimated by Xanthos et al. [4] when PP interfaces with SEEPS midblock, instead of directly with PS. The interfacial tension reduction is from 4.3 to 0.29 mN/m, and the interfacial thickness increase is from 0.7 to 11.6 nm [4].

Therefore, the SEEPS block copolymer will be adsorbed preferentially at the interfaces between the domains of homopolymers PS and PP, reducing the interfacial tension and enhancing the interfacial adhesion and strength. As a result, the size of the dispersed phase domains, i.e. PS domains, in the compatibilized nonporous precursor films is much smaller than the noncompatibilized one [4]. When these precursor films are subject to uniaxial drawing, the resulting microvoids along the PP/SEEPS midblock interface have a much shorter length due to the reduced dispersed domain size and the enhanced interfacial adhesion. This is indeed the result of our SAXS analysis. The length of the microvoids drops from 471 ± 100 nm (line 1 of Table 2) to some 200 nm (line 2, 3 and 4 of Table 2) when the SEEPS block copolymer is used as a compatibilizer.

However, increasing compatibilizer concentration from 90/10/5 to 85/15/7.5 (wt%) does not lead to an even smaller microvoids length. Instead, the length of microvoids increases from 174 ± 11 to 215 ± 16 nm. It appears that when the block copolymer concentration increases to 85/15/7.5, the block copolymer tends to concentrate at the interface of the PS domains to form a cluster and produce aggregates of a composite PS/SEEPS dispersed phase [2,4]. This leads to reduced interfacial adhesion and strength. It is for this reason that an increase in microvoids length is observed when the block copolymer concentration increases from 90/10/5 to 85/15/7.5 (wt%). Therefore, the composition 90/10/5 gives rise to the best interfacial adhesion and strength. This is shown on lines 3 and 4 of Table 2.

4.2. The effect of mixing protocol

For the block copolymer to perform its function of compatibilization, it has to be located at the interface between the domains of homopolymers PP and PS. A judicious choice of a processing condition should promote the diffusion of the block copolymer into the interface of PP and PS during extrusion. The mixing protocol is found to be the most important processing factor that determines the distribution of the block copolymer SEEPS between the PP and PS domains. Compared to the one-step mixing protocol, the two-step mixing protocol, i.e. premixing SEEPS and the minor component PS before mixing with the major component PP, apparently allows a better distribution of the block copolymer SEEPS at the interface and gives rise to a smaller length of the microvoids upon

drawing. The reduction in microvoids length is from 205 ± 15 to 174 ± 11 nm. This is shown on lines 2 and 3 of Table 2.

Therefore, among all films made from ternary blends, the film PP/PS/SEEPS-90/10/5-2 has the best interfacial adhesion and strength and the shortest microvoids length (174 ± 11 nm). The films PP/PS/SEEPS-90/10/5-1 and PP/PS/SEEPS-85/15/7.5-2 has roughly the same interfacial adhesion and strength, and their microvoids length are 205 ± 15 nm and 215 ± 16, respectively.

4.3. The interconnectivity of the microvoids

One of the most important parameters of a membrane is its transport property. Shown in Fig. 5 is the methanol permeability of these porous films measured by Chandavasu, Xanthos, Sirkar and coworkers [2,4]. The porosity measured by Chandavasu, Xanthos, Sirkar and coworkers [2,4] and microvoids dimensions computed in this paper are shown in the legends. From Fig. 5, it is obvious that for a specific driving force (i.e. pressure), the higher the porosity, the higher the methanol permeability.

Given the monotonic dependence of the membrane transport property on porosity, the question as to what other membrane characteristics will affect its transport property can be clearly posed. For membranes with the same pore geometry and porosity, fabricated from the same process and material, the interconnectivity among pores is probably the next important characteristic that determines the transport property of a membrane.

A simple approach to quantify the interconnectivity among pores is proposed. With the use of the data from Fig. 5, a plot of methanol permeability under a specific driving force (in this case, $P = 80$psi) with respect to the porosity for each film studied in this paper is generated in Fig. 6. A straight line is drawn between the origin and each point in Fig. 6. Each line stands for the change of methanol permeability as a function of porosity at a constant degree of interconnectivity, which is equal to that of the film represented by the marker, through which the line is drawn. Therefore, the degree of interconnectivity for each film can be represented by the slope of the corresponding straight line: the larger the slope, the better the interconnectivity. In order for this approach to be valid, it is assumed that membranes are made from similar or the same materials using the same process, and have the same pore geometrical shape.

From Fig. 6, it is interesting to observe that the degree of interconnectivity of the films studied in this research is in line with the interfacial adhesion and strength discussed in Sections 4.1 and 4.2, and the length of the microvoids can also be used as a measure for the degree of interconnectivity. As discussed above, for interfacial adhesion and strength, PP/PS-90/10-1 < PP/PS/SEEPS-90/10/5-1 ≈ PP/PS/SEEPS-85/15/7.5-2 < PP/PS/SEEPS-90/10/5-2. The same trend is observed for the degree of interconnectivity as represented by the line slopes in Fig. 6, i.e. the shorter the microvoids length, the higher the degree of interconnectivity, and the larger the line slope. The degrees of connectivity for PP/PS/SEEPS-90/10/5-1 and PP/PS/SEEPS-85/15/7.5-2 are very close to each other. Note that the broken line connects the origin to PP/PS/SEEPS-85/15/7.5-2, which is represented by a closed circle in Fig. 6.

Nevertheless, the degrees of interconnectivity of the ternary blends are close to one another, and are much higher than that of the film made from the binary blends. Are their porous structures significantly different from those of the binary film?

When comparing the SAXS patterns of the films studied in this research as shown in Fig. 7, one observes scattering streaks around the beamstop without an equatorial orientation for films made from ternary blends. These streaks will be termed non-equatorial streaks. Around the beamstop, the non-equatorial streaks join together. The streaklike character can be observed at the edge of each non-equatorial streak marked in Fig. 7.

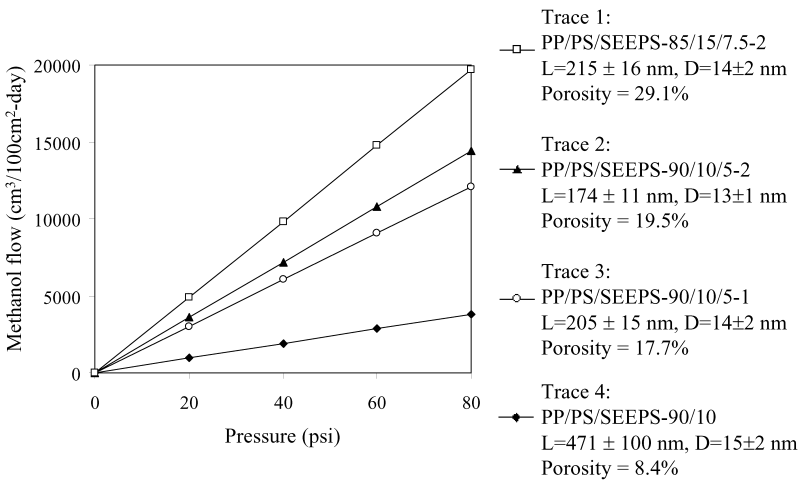

Fig. 5. A plot of permeability of methanol through the binary and ternary blends (from Ref. [2]) with the corresponding microvoids dimensions and porosity (from Ref. [2]).

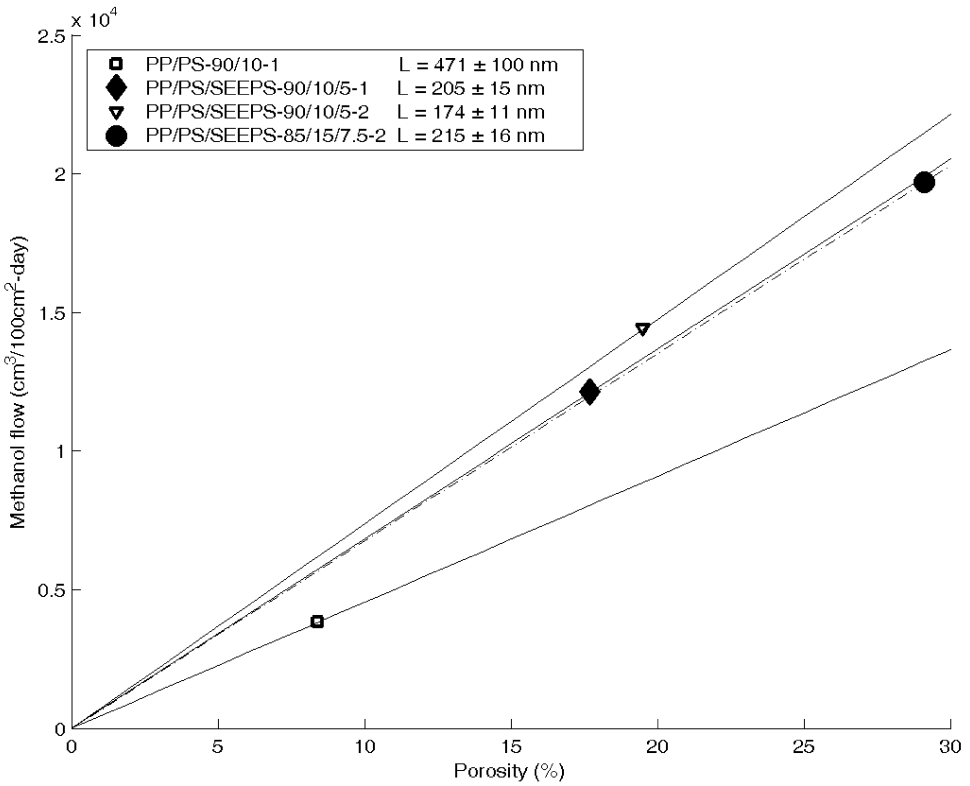

Fig. 6. A plot for evaluating the degree of interconnectivity among microvoids in membranes with similar pore geometry and made from similar materials and processes.

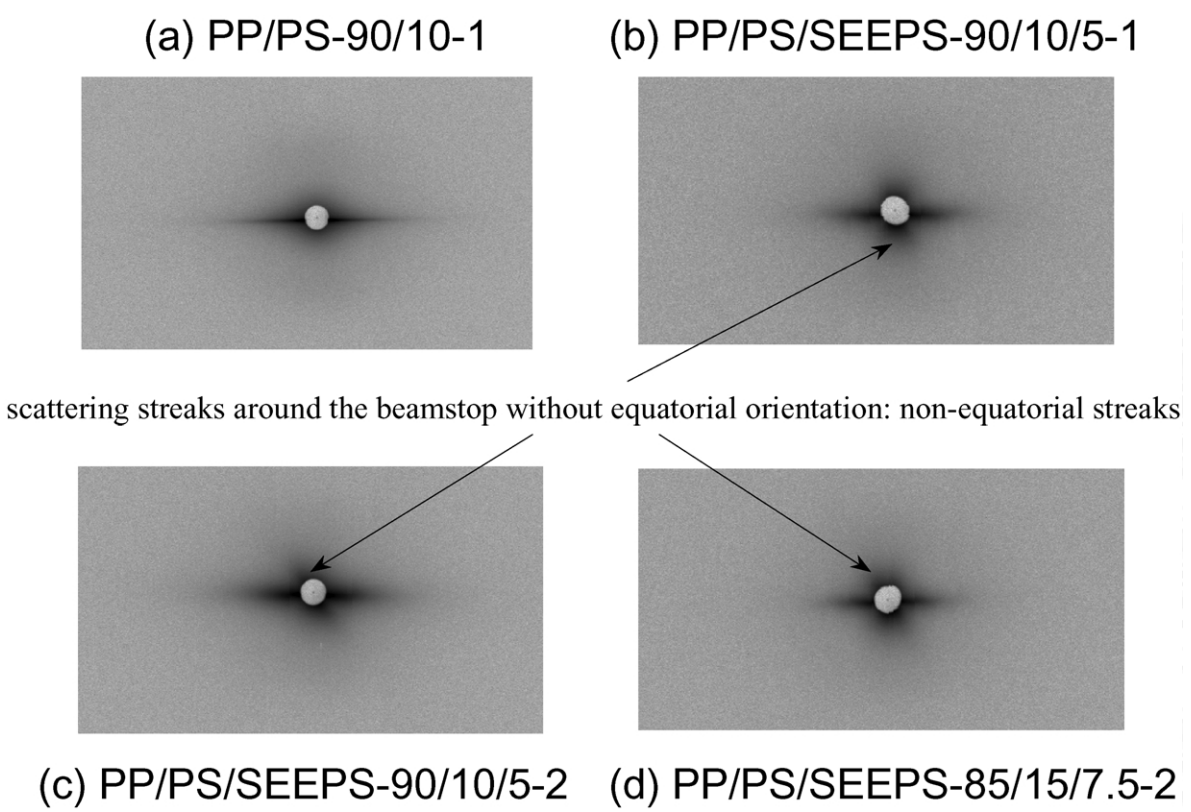

Fig. 7. Two-dimensional small-angle X-ray scattering patterns from PP/PS binary and ternary blends, (a) from PP/PS-90/10-1, (b) from PP/PS/SEEPS-90/10/5-1, (c) from PP/PS/SEEPS-90/10/5-2, (d) from PP/PS/SEEPS-85/15/7.5-2.

Comparing parts (a)–(d) of Fig. 7, one observes that only part (a), i.e. the pattern from the PP/PS binary blends, does not bear the non-equatorial streaks. The non-equatorial streaks are likely originated from the 'bridging microvoids', which do not oriented preferentially along the draw direction. These bridging microvoids, which are responsible for the interconnectivity among microvoids, have a complex orientation and geometry, which is evident from the irregular shape of non-equatorial streaks shown in Fig. 7. For films made from ternary blends, their degree of interconnectivity are similar due to the existence of 'bridging microvoids'.

To the author's knowledge, this is the first time that a measure of the degree of interconnectivity is defined, and that the non-equatorial scattering streaks are ascribed to the interconnecting microvoids, i.e. the 'bridging microvoids', which have a complex geometry and orientation. The computational procedures to assess the non-equatorial streaks are being developed.

5. Conclusions

Intense equatorial streaks of SAXS patterns from immiscible PP/PS binary and PP/PS/SEEPS ternary blends subject to uniaxial drawing are attributed to the scattering from uniaxially oriented microvoids. The length of the microvoids is identified as an effective measure of the interfacial adhesion and strength between phase domains. The initial addition of compatibilizer (PP/PS/SEEPS of 90/10/5 wt%) enhances interfacial adhesion and reduces microvoids length. Further addition of compatibilizer (PP/PS/SEEPS of 85/15/7.5 wt%) leads to the formation of clusters and aggregates of a composite PS/SEEPS dispersed phase, giving rise to a larger microvoids dimension. Comparing to the one-step mixing protocol, the two-step mixing protocol allows a better distribution of the compatibilizer between interfaces of PP/PS domains, giving rise to a smaller microvoids length.

The transport property of the films is are largely determined by porosity and the degree of interconnectivity among the microvoids. A convenient measure of the degree of interconnectivity is proposed. The degrees of interconnectivity of these films are in accordance with the interfacial adhesion and strength. The non-equatorial streaks are observed and attributed to the microvoids with a complex orientation and geometry, which are responsible for the interconnectivity among microvoids. Computational procedures to evaluate the non-equatorial streaks are being developed.

6. Supplementary material

The computation of this work is implemented in the computational environment of MATLAB (Mathworks, Inc., MA). Source codes are available upon request.

Acknowledgements

JW is much indebted to Professors Marino Xanthos and Kamalesh Sirkar for providing samples. JW also acknowledges the financial support by SBR Grant Program of New Jersey Institute of Technology, Grant No. 421880.

References

[1] Paul DR. Chapter 1: Polymer blends: phase behavior and property relationships. In: Paul DR, Sperling LH, editors. Multicomponent polymer materials. Washington, DC: American Chemical Society; 1986.
[2] Chandavasu C. Microporous Polymeric Membranes via Melt Processing. Newark, NJ: Department of Chemical Engineering, New Jersey Institute of Technology; 2001.
[3] Chandavasu C, Xanthos M, Sirkar KK, Gogos CG. Polymer 2002;43:781.
[4] Xanthos M, Chandavasu C, Sirkar KK, Gogos CG. Polym Eng Sci 2002;42(4):810.
[5] Guinier A, Fournet G. Small-angle scattering of X-rays. New York: Wiley; 1955.
[6] Grubb DT, Prasad K. Macromolecules 1992;25:4575.
[7] Wu J, Schultz JM, Yeh F, Hsiao BS, Chu B. Macromolecules 2000;33:1765.
[8] Statton WO. J Polym Sci 1956;22:385.
[9] Statton WO. J Polym Sci 1962;58:205.
[10] Ruland W. J Polym Sci, Polym Symp 1969;28:143.
[11] Ruland W, Perret R. J Appl Crystallogr 1969;2:209.
[12] Ruland W, Perret R. J Appl Crystallogr 1970;3:525.
[13] Murthy NS, Reimshuessel AC, Kramer V. J Appl Polym Sci 1990;40:249.
[14] Murthy NS, Bednarczyk C, Moore RAF, Grubb DT. J Polym Sci: Part B: Polym Phys 1996;34:821.
[15] Kulashreshtha AK, Rao MVS, Dweltz NE. J Appl Polym Sci 1985;30:3423.
[16] Hoogsteen W, Pennings AJ, Brinke G. Colloids Polym Sci 1990;268:245.
[17] Hoogsteen W, Brinke G, Pennings AJ. J Mater Sci 1990;25:1551.
[18] Tang MY, Fellers JF, Lin JS. J Polym Sci, Polym Phys Ed 1984;22(12):2215.
[19] Marquardt DW. J Soc Ind Appl Math 1963;11:431.
[20] Kratky O. Chapter 1: A survey. In: Glatter O, Kratky O, editors. Small-angle X-ray scattering. London: Academic Press; 1982.
[21] Xanthos M. Polym Eng Sci 1988;28:1392.